14th World Congress on Computational Mechanics (WCCM)
ECCOMAS Congress 2020
Virtual Congress: 11-–15 January 2021
F. Chinesta, R. Abgrall, O. Allix and M. Kaliske (Eds)

NUMERICAL ANALYSIS OF VISCOELASTIC FLUID INJECTION PROCESSES

Ahmad Amani[1*], Eugenio Schillaci[2], Deniz Kizildag[1], Carlos David Pérez-Segarra[1]

[1] Heat and Mass Transfer Technological Center (CTTC),
Universitat Politécnica de Catalunya-Barcelona Tech (UPC),
ESEIAAT, Colom 11, 08222 Terrassa (Barcelona), Spain. ahmad.amani@upc.edu

[2] Termo Fluids S.L. Avda Jacquard 97 1-E, 08222 Terrassa (Barcelona), Spain
http://www.termofluids.com

Key words: Direct Numerical Simulations (DNS), Viscoelastic Liquids, Injection Processes, 3D printers

Abstract. In this work, a numerical framework aimed at simulating high-viscous and viscoelastic liquid injection processes is presented. The study of fluid injection with viscoelastic properties, such as synthetic polymers, is of great importance in several industrial sectors, such as metallurgy, automotive, food and pharmaceutical products, ink jets and 3D printers. In this work, a Geometrical Volume-of-Fluid (VOF) method is used to represent the interface, while finite-volume discretizations of Navier-Stokes equations on collocated unstructured meshes are solved through a fractional step method. Viscoelastic constitutive models are used to resolve the non-Newtonian behaviours. The employed implementations allow integrating different types of constitutive equations and stabilization approaches. The test case proposed in the current work consist of the simulation of the discharge of a polymeric jet from an upper nozzle into an air-containing cavity with solid bottom. The behavior of the fluids under analysis is validated by observing the onset of fluid-buckling structures. This phenomenon consists in the appearance of toroidal oscillation (as coiling and folding patterns) after the jet hits the solid surface and begins to accumulate. First, low-Reynolds number (Re$<$1.0) Newtonian Jets are analyzed, with the objective of validating the appearance of buckling as a function of Re number, and comparing the results with reference works. Finally, the potentialities of the proposed numerical methods are shown by simulating buckling phenomena in viscoelastic Jets described with the Oldroyd-B constitutive model.

1 INTRODUCTION

The numerical simulation of low-Reynolds number flow injection processes can provide valuable information about various industrial processes, such as injection molding, ink jet printing and 3D printing by means of polymeric inks. Moreover, numerous processes which involve similar phenomenologies are present in the food-processing industry. While viscous fluids strain uniformly when a stress is applied, elastic solids strain instantaneously. Consequently, viscoelastic fluids exhibit time-dependent strain, i.e. when a stress is applied, their strain approaches its equilibrium value on a time-scale which is a characteristic of the fluid. The modeling and simulation of this kind of processing operations appears as a fundamental tool, which leads to a better understanding of how the rheological properties of polymers affect their processability, and reducing the time and costs related to the processes and the final products. The development of accurate numerical tools for the simulation of viscoelastic multiphase flows is vital

from both fundamental and practical points of view. Historically, the main challenges to be faced in the modeling of injection processes by means of finite-volume based solvers consist of: (1) the correct modeling of the viscoelastic behavior apparent in many of the aforementioned applications; (2) the correct representation of the interface that divides the injected fluid and the surrounding gas.

The accurate simulation of the viscoelastic properties of the fluid passes through the choice of the constitutive model suitable to represent the polymeric material in question, whose behavior depends on a non-linear combination of its viscous and elastic properties. Some of the most common constitutive models as the Oldroyd-B, Giekus and FENE type models, have already been successfully implemented in finite-volume formulations. Several examples are present in the literature regarding their implementations for multiphase applications. Between the infinitely extensionable models, the Giekus model [1, 2] has generally given good results in the simulation of polymers, as well as the Oldroyd-B model implementation [3]

Regarding the representation of the interface, the Level-Set and Volume-of-Fluid (VoF) methods are nowadays the most widely used approaches in simulation packages. A third alternative, consists in the Front-Tracking (Marker-and-Cell) method. The effectiveness of these methods has already been demonstrated in the simulation of high-viscous Newtonian and viscoelastic flows in various configurations. In VoF methods [4], the advected function is the volume fraction scalar field of one of the phases. Its value is 1 or 0 in the cells totally filled by that phase or totally empty, while it varies from 0 to 1 in the interface zone, where the cells are partially filled by the two phases. Between the others, Favero et al. [1] used the VoF method embedded in OpenFoam to study viscoelastic multiphase flow problems, by employing the Giekus constitutive model. Bonito et al. [5] assessed the appearance of buckling in 2D and 3D Jets, respectively. A disadvantage of the VOF method is its difficulty in computing accurate geometrical properties (interface normal and curvature) from the volume fraction function as it presents a step discontinuity. Alternatively, in the Level-Set Method (LSM) [6] the interface is identified by the zero contour of a signed level-set function, advected at every time step. Employing this approach, Ville et al. [7] carried out simulations of fluid injection for square and rectangular inlets. The major defect of LSM is due to the discrete solution of transport equations which leads to numerical errors in conservation of mass of the fluid-phase. In the Marker-and Cell method the individual interfaces are represented by sets of connected marker points. Despite being quite inefficient when complex interfacial break-up and coalescence occur, this approach appear particularly effective in implementing free-surface approximations, where the effect of the gas is neglected, and representing phenomena, as the fluid buckling, with limited break-up. Tome et al. [8] proved the ability of their updated MAC method on capturing physical instabilities regarding the buckling of planar jets with high-viscous and viscoelastic properties.

The fluid buckling phenomenon is a challenging case usually employed to test the capability of numerical models to effectively represent the behavior of high-viscous and viscoelastic fluids. The case consists in simulating a jet injected downwards, under the effect of gravity, into a parallelepiped cavity. After hitting the solid base of the box, oscillations may appear on the free-surface of the jet, which eventually lead to coiling and folding patterns. Regarding a high-viscosity and axysimmetric Newtonian jet, Cruickshank and Munson [9] quoted relationship indicates buckling for:

$$Re < 1.2 \quad \text{and} \quad H/D > 7 \tag{1}$$

with $Re = \rho UD/\mu$, where ρ and μ are the density and viscosity of the jet, respectively, and U, is the injection velocity. H/D is the aspect ratio of the cavity, describing the ratio of the cavity height to the

(hydraulic) diameter of the inlet. Tome and McKee [8] performed simulations on 2D planar viscous jets and obtained the following best-fit relationship which relates the Reynolds number at which buckling appears with aspect ratio of the cavity:

$$\mathrm{Re}^2 \leq \frac{1}{\pi}\frac{(H/D)^{2.6} - 8.8^{2.6}}{(H/D)^{2.6}} \tag{2}$$

In this work, direct numerical simulation of the Navier-Stokes equations is used for two-phase flow where the interface evolution is captured using a volume-of-fluid method. The approach presented by Amani et al. [3] for the resolution of non-Newtonian fluids is used, while the set-up presented by Schillaci et al. [10] for liquid injection simulations at high Re is employed to fix boundary inlet and outlet conditions. The rest of the paper is organized as follows: mathematical formulation are presented in Section 2, numerical methods are described in Section 3. The numerical set-up is presented in Section 4, followed by the numerical results and discussion. Finally, conclusion remarks are provided in Section 5.

2 Mathematical Formulations

The numerical framework employed in this work accounts for a finite-volume discretization of Navier-Stokes equations for mass and momentum conservation on collocated unstructured meshes, Volume-of-Fluid description of the interface and constitutive models to take into account viscoelastic properties of the solutes. A Volume-of-Fluid interface capturing approach is used to evaluate the time-evolution of the moving interface. In this approach, the interface is captured implicitly using a scalar field $\alpha(\mathbf{x},t)$, representing the volume fraction of a phase inside each cell of the discretized domain at a given time. Cells with $0 < \alpha(\mathbf{x},t) < 1$ are known as interface cells; $\alpha(\mathbf{x},t)$ is equal to 1 if the cell is filled with associated phase and 0 otherwise. For a given velocity field obtained from the Navier-Stokes equations, the motion of the interface is solved by an advection equation as:

$$\frac{\partial \alpha(\mathbf{x},t)}{\partial t} + \nabla \cdot (\alpha(\mathbf{x},t)\mathbf{u}) = 0. \tag{3}$$

A piecewise linear interface calculation (PLIC) method started by the work of DeBar [11] is used to geometrically reconstruct the interface as planes with an arbitrary orientation in each interface cell. In this method, regardless of the grid cell type, i.e. structured or unstructured, the interface in each cell is defined as:

$$\mathbf{x} \cdot \mathbf{n} - d = 0 \tag{4}$$

where $\mathbf{n}$ is the unit-normal vector pointing outward with respect to the phase $\alpha(\mathbf{x},t)$, $\mathbf{x}$ is the position vector of a point on the interface and d is the signed distance from the origin to the plane. In this work, a point-cloud approach is used to evaluate the normal vectors of the interface cells.

The velocity scalar field, $\mathbf{u}(\mathbf{x},t)$, needed for the advection of the interface, is derived from the resolution of Navier-Stokes equations in the incompressibility and variable properties limit (density, viscosity). In a domain occupied by two incompressible and immiscible fluids separated by an interface, the velocity and pressure fields are governed by the following equations:

$$\frac{\partial}{\partial t}(\rho\mathbf{u}) + \nabla \cdot (\rho\mathbf{u}\mathbf{u}) = -\nabla p + \nabla \cdot \tau + \rho\mathbf{g} + \sigma\kappa\mathbf{n}\delta_\Gamma \tag{5}$$

$$\nabla \cdot \mathbf{u} = 0 \tag{6}$$

Some of the cases analyzed in this work deal with high-viscous Newtonian fluids, hence, the stress tensor is simply evaluated as:

$$\tau = \mu\left(\nabla\mathbf{u} + (\nabla\mathbf{u})^T\right) \tag{7}$$

On the other hand, when the fluid under study is viscoelastic, the stress tensor includes the responses from the solvent and the polymeric solute as:

$$\tau = \tau_s + \tau_p \tag{8}$$

where the response of the solvent, τ_s, is evaluated as follows:

$$\tau_s = \mu_s(\dot{\gamma})\left(\nabla\mathbf{u} + (\nabla\mathbf{u})^T\right) \tag{9}$$

In this formulation, the solvent's apparent viscosity μ_s could be described as a function of shear-rate tensor $\dot{\gamma}$ in the context of Generalized Newtonian Fluid (GNF) formulation. However, in the current study, the value of μ_s is considered to be constant. On the other side, the polymeric contribution of the stress response is evaluated as:

$$\tau_p = \frac{\mu_p}{\lambda_1} f_s(c) \tag{10}$$

where $f_s(c)$ is a strain function depending on the constitutive model, and c is the conformation tensor, an internal tensorial variable representing the macromolecular configuration of the polymeric chain. The basic mechanism for stress build-up and relaxation is governed by a differential equation of the conformation tensor as:

$$\frac{Dc}{Dt} = \nabla\mathbf{u}^T \cdot c + c \cdot \nabla\mathbf{u} - \frac{1}{\lambda_1} f_s(c) \tag{11}$$

In this work, the Oldroyd-B model [12] is adopted for the representation of $f_s(c)$ as used by Amani et al. [3]. A continuum surface force (CSF) approach [13] is used to transform the surface tension force into a volume force. The density, viscosities (μ_s and μ_p), and relaxation time can be defined as scalar-fields inside the whole domain as follows:

$$\zeta = \zeta_1 H + \zeta_2(1-H) \tag{12}$$

where $\zeta \in \{\rho, \mu_s, \mu_p, \lambda_1\}$ and H is the Heaviside step function which takes the value one in dispersed phase and zero elsewhere.

3 Numerical Method

The numerical methods are implemented in an in-house parallel c++/MPI code called TermoFluids [14]. Validations and verifications of the numerical methods used in this work have been reported in [15, 16, 17, 10, 18, 3, 19, 20, 21]. The Finite-volume (FV) approach is used to discretize the Navier-Stokes and VOF equations on a collocated grid, so all the computed variables are stored at cell centroids.

The algorithm employed to solve the governing equations described in Section 2 at each time-step can be described as follows:

1. Physical properties, interface geometric properties and velocity fields are initialized (only first iteration).

2. Allowable time step is calculated. The value of Δt is limited by CFL conditions on convective term and also by explicit treatment of surface tension as used by [18]. To decrease the computational costs, the maximum value of the CFL coefficient which leads to a stable simulation is used.
3. Using the evaluated normal vectors at the interface cells, the value of the d parameter in Equation 4 is calculated using the Brent's root-finding algorithm [22], thus, locating the interface planes of PLIC method at each interface cell.
4. In the context of finite-volume methods, the application of the divergence theorem and the spatial discretization of this equation over a cell with volume ∂v and face set F with area vectors of $d\mathbf{A}_f$ results to:

$$\int_{\partial v} \frac{\partial \alpha(\mathbf{x},t)}{\partial t} + \sum_{f_i \in F} (\alpha(\mathbf{x},t)\mathbf{u})_f \cdot d\mathbf{A}_{f_i} = 0 \tag{13}$$

   where the first term deals with the temporal evolution of the interface and the second term evaluates the total volumetric flux of the phase represented by volume-fraction function $\alpha(\mathbf{x},t)$ across the faces of the associated grid cell in a timestep based on the selected temporal scheme. A geometrical approach as presented by Jofre et al. [15] is used to evaluate the second term by employing the geometrically reconstructed interface calculated based on volume fraction values at interface cells. In the classical formulation, the curvature is calculated as divergence of the gradient of color-function: $\kappa = \nabla \cdot (\nabla\alpha(\mathbf{x},t)/|\nabla\alpha(\mathbf{x},t)|)$. However, given the fact that the color-function in VOF is discontinuous by definition, applying derivative type operations to this discontinuous function leads to numerical errors. To circumvent this issue, a sign distance function (ψ) representing the minimum distance of each cell's center from the PLIC interface is evaluated in a neighbouring area of the interface. The curvature is then calculated using this continuous auxiliary distance-function as: $\kappa = \nabla \cdot (\nabla\psi/|\nabla\psi|)$.
5. Physical properties in the domain (density, solvent and polymeric viscosities, relaxation time) and geometrical properties at the interface (curvature and interface normal) are updated from the advected color-function $\alpha(\mathbf{x},t)$ as described in Equation 12.
6. The conformation tensor is calculated by solving the constitutive equation of Equation 11. An important numerical issue related to numerical resolution of viscoelastic materials is due to the stiff hyperbolic nature of the constitutive equations, which make them prone to numerical instabilities and eventually to the blow-up of the numerical solution. This problem arises when the Weissenberg number (Wi) of the problem exceeds a critical value (usually around one). The log-conformation representation method [23] is employed as stabilization approach for the discretization of the constitutive equation and to circumvent the High Weissenberg Number Problem (HWNP). Further details about the numerical implementations of constitutive models are given in [3].
7. A semi-implicit fractional step projection method is used to solve the velocity-pressure coupling. In high-viscosity/non-Newtonian fluids, the varying value of viscosity can increase dramatically and lead to excessively small time-steps of the simulation and thus resulting in huge computational costs. To circumvent this issue, the diffusion term in equation 5 is treated implicitly. The proposed discretization for the predictor step was already presented and employed by the authors in [3, 16].

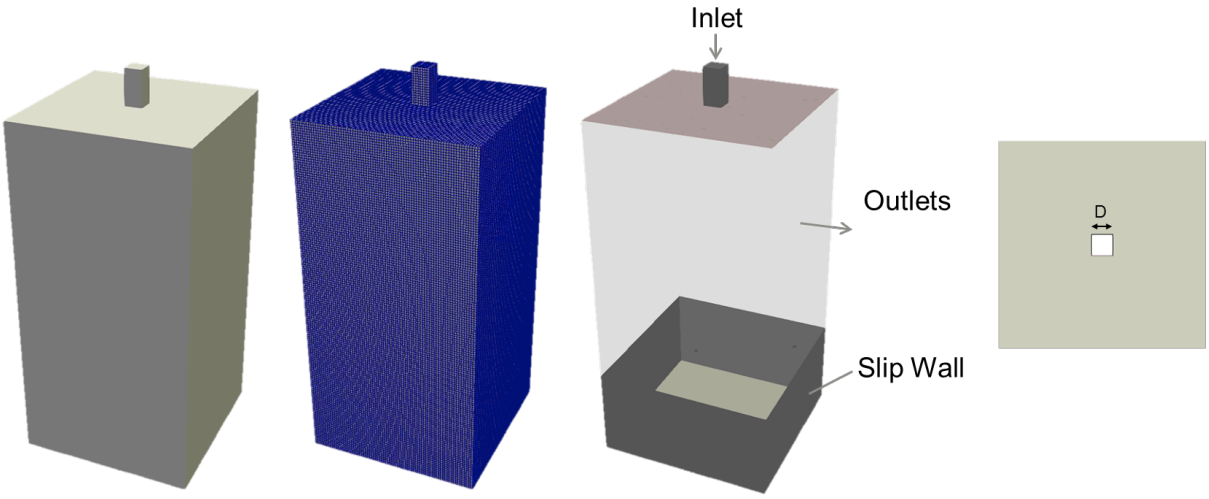

Figure 1: Numerical set-up used in this work for the simulation of the jet injection.

8. A correction to the predicted velocity applies as below:

$$\frac{\rho \mathbf{u}^{n+1} - \rho \mathbf{u}^{*}}{\Delta t} = -\nabla_h p^{n+1} \tag{14}$$

9. Poisson equation reads as follows and is solved using a preconditioned conjugated gradient method:

$$\nabla_h \cdot \left(\frac{1}{\rho} \nabla_h (p^{n+1}) \right) = \frac{1}{\Delta t} \nabla_h \cdot (\mathbf{u}^{*}) \tag{15}$$

10. The velocity $\mathbf{u}^{n+1}$ is corrected by the updated pressure as:

$$\mathbf{u}^{n+1} = \mathbf{u}^{*} - \frac{\Delta t}{\rho} \nabla_h (p^{n+1}) \tag{16}$$

4 Numerical experiments and discussion

The test case analyzed in the current work consist of a low Reynolds number injection of liquid l into a rectangular box filled by quiescent gas g. The numerical set-up, depicted in Fig. 1, consists of a rectangular box, where a heavier fluid is injected from a square shaped inlet of dimension D (hydraulic diameter) with a constant inlet velocity, u_l . The rectangular box has height H equal to $20D$. No-slip boundary conditions are applied at the base and on the lateral bottom surfaces to allow the fluid deposition at the bottom. An outlet pressure is imposed at the other boundaries in order to represent the outflow conditions, allowing the gas to go out of the domain as the liquid jet is being injected. The properties of the fluids are specified in each section. The domain is discretized into (80, 80, 160) cubic cells in laterals and vertical directions, hence, a structured mesh is employed. As mentioned in Section 1, and according to Equation 2, for a H/D ratio of 20, as employed in the simulations of this section, one can expect buckling of a Newtonian jet as long as the Reynolds number is smaller than 0.53. To check the

Figure 2: Evolution of a Newtonian Jet in a domain with H/D=20 for three different Reynolds numbers of (left column) 0.2, (middle column) 0.5, and (right column) 0.7.

Figure 3: Evolution of a viscoelastic jet in a domain with H/D=20, Re=0.5 and Wi=0.1.

accuracy of our numerical tools in capturing the buckling phenomena, we perform the simulations of injection of a Newtonian jet into a domain with H/D=20, with different Reynolds numbers of 0.2, 0.5, and 0.7.

Figure 2 shows the evolution of the injected jet for the three given Reynolds numbers. Regardless of the time scale of the problem, we are here exclusively interested in analyzing the evolution of the free surface during the discharge process. On the left side three different time instants of the jet evolution of the Re=0.2 case are reported. The injected liquid starts to fold immediately once it reaches the cavity floor. Hence, toroidal oscillations appear and the jet starts to coil into itself with a regular frequency. A similar process is noticed in the center pics, where the results of the case with Re=0.5 are reported. After the initial folding, the jet starts to coil with a regular frequency as well. On the other hand, for the case with Re = 0.7 (right column) the jet begins to expand uniformly once it reaches the bottom wall. Due to the high viscosity, however, no break-up process of the free surface is visible, which will tend to fill the vessel on a regular basis. Resuming, the case with Re=0.2 and 0.5 illustrates the buckling while the case with Re=0.7 ends up with the uniform distribution of the liquid in bottom plane. This agrees with the expected evolution based on the reported results in [8] and the relationships of Equation 2, which predicts the onset of buckling for Re$<$0.53.

Figure 3 illustrates the time evolution of a viscoelastic (Oldroyd-B) jet with non-dimensional Reynolds and Weissenberg numbers of $Re = \rho UD/\mu_0 = 0.5$ and $Wi = \lambda_1 U/D = 0.1$, respectively, where μ_0 is the total viscosity of the liquid defined as summation of polymeric and solvent viscosities: $\mu_0 = \mu_s + \mu_p$. Even though the Weissenberg number, which describes the elastic forces to the viscous forces in the flow is small (0.1), it is big enough to cause instabilities in the jet, deflecting it from its symmetric evolution prior to colliding the bottom wall. For this case, the jet still ends up coiling after the collision with the bottom wall.

5 Conclusion

This paper presents the results obtained in the simulation of Newtonian and non-Newtonian jets characterized by low speed and high viscosity, and therefore, by Reynolds number lower than 1.0. An effective and validated numerical method of this type contributes considerably to the study the rheological properties of polymeric fluids (and their discharge process), in particular, those related to 3D printing processes. The numerical method presented incorporates the finite-volume based/direct numerical simulation of the Navier-Stokes equations for a multiphase flow consisting of a fluid and a gas. The transport of the interface is carried out through a geometrical VoF method. The following techniques are used to solve numerical problems related to the simulation of non-Newtonian and/or high viscosity flows: (1) a particular sign distance function is employed in the calculation of the curvature in order to avoid numerical errors due to the discontinuity of the VoF function; (2) a semi-implicit fractional step projection method is used to solve the velocity-pressure coupling, in order to circumvent the Low Viscosity Ratio Problem; (3) The log-conformation method is employed as stabilization approach for the discretization of the constitutive equation, in order to circumvent the High Weissenberg Number Problem. The numerical framework is validated by assessing the appearance of fluid-buckling for $Re<0.53$ in Newtonian flows, as indicated by the literature. Hence, the potentialities of the model are expressed by simulating the discharge process and fluid-buckling in a viscoelastic (Oldroyd-B) fluid.

Acknowledgments

This work was developed in the context of a research project (BASE3D 001-P-001646) co-financed by the European Union Regional Development Fund within the framework of the ERDF Operational Program of Catalonia 2014-2020 with a grant of 50% of total cost eligible. The work has also been financially supported by a competitive R+D project (ENE2017-88697-R) of the Spanish Research Agency. The author E.Schillaci acknowledges the financial support of the Programa Torres Quevedo (PTQ2018-010060).

References

[1] J. L. Favero et al. “Viscoelastic fluid analysis in internal and in free surface flows using the software OpenFOAM”. In: *Computers and Chemical Engineering* 34 (2010), pp. 1984–1993.

[2] M. F. Tomé et al. “Numerical solution of the Giesekus model for incompressible free surface flows without solvent viscosity”. In: *Journal of Non-Newtonian Fluid Mechanics* 263 (Jan. 2019), pp. 104–119.

[3] A. Amani et al. “A numerical approach for non-Newtonian two-phase flows using a conservative level-set method”. In: *Chemical Engineering Journal* 385 (Apr. 2020), p. 123896.

[4] C. W. Hirt and B. D. Nichols. “Volume of fluid (VOF) method for the dynamics of free boundaries”. In: *Journal of Computational Physics* 39.1 (1981), pp. 201–225.

[5] A. Bonito, M. Picasso, and M. Laso. “Numerical simulation of 3D viscoelastic flows with free surfaces”. In: *Journal of Computational Physics* 215.2 (2006), pp. 691–716.

[6] S. Osher and J. A. Sethian. “Fronts propagating with curvature-dependent speed: algorithms based on Hamilton-Jacobi formulations”. In: *Journal of Computational Physics* 79.1 (1988), pp. 12–49.

[7] L. Ville, L. Silva, and T. Coupez. "Convected level set method for the numerical simulation of fluid buckling". In: *International Journal for Numerical Methods in Fluids* 66.3 (2011), pp. 324–344.

[8] M. F. Tome and S. McKee. "Numerical simulation of viscous flow: Buckling of planar jets". In: *International Journal for Numerical Methods in Fluids* 29.6 (1999), pp. 705–718.

[9] J. O. Cruickshank and B. R. Munson. "Viscous Fluid Buckling Of Plane And Axisymmetric Jets". In: *Journal of Fluid Mechanics* 113.-1 (Dec. 1981), pp. 221–239.

[10] E. Schillaci et al. "A numerical study of liquid atomization regimes by means of conservative level-set simulations". In: *Computers & Fluids* 179 (2019), pp. 137–149.

[11] R. B. DeBar. "Fundamentals of the KRAKEN code". In: *Technical Report* (1974).

[12] J. G. Oldroyd. "On the Formulation of Rheological Equations of State". In: *Proceedings of the Royal Society A: Mathematical, Physical and Engineering Sciences* 200.1063 (1950), pp. 523–541.

[13] J. U. Brackbill, D. B. Kothe, and C. Zemach. "A continuum method for modeling surface tension". In: *Journal of Computational Physics* 100.2 (1992), pp. 335–354.

[14] *Termo Fluids S.L.*

[15] L. Jofre et al. "A 3-D Volume-of-Fluid advection method based on cell-vertex velocities for unstructured meshes". In: *Computers and Fluids* 94 (2014), pp. 14–29.

[16] A. Amani et al. "Numerical study of droplet deformation in shear flow using a conservative level-set method". In: *Chemical Engineering Science* 207 (2019), pp. 153–171.

[17] E. Schillaci et al. "A low-dissipation convection scheme for the stable discretization of turbulent interfacial flow". In: *Computers & Fluids* 153 (2017), pp. 102–117.

[18] A. Amani et al. "Numerical study of binary droplets collision in the main collision regimes". In: *Chemical Engineering Journal* (2019), pp. 477–498.

[19] E. Gutiérrez et al. "Numerical approach to study bubbles and drops evolving through complex geometries by using a level set-Moving mesh-Immersed boundary method". In: *Chemical Engineering Journal* 349.February (2018), pp. 662–682.

[20] A. Amani et al. "A Study on Binary Collision of GNF Droplets Using a Conservative Level-Set Method". In: *7th European Conference on Computational Fluid Dynamics (ECFD 7)*. Glasgow, UK, 2018.

[21] A. Amani et al. "DNS of un-equal size droplets collision using a moving-mesh/level-set method". In: *ERCOFTAC workshop direct and large eddy simulation 12 (DLES 12)*. Madrid, Spain, 2019.

[22] G. Ermentrout. "Numerical recipes in C". In: *Mathematical Biosciences* (1989).

[23] R. Fattal and R. Kupferman. "Constitutive laws for the matrix-logarithm of the conformation tensor". In: *Journal of Non-Newtonian Fluid Mechanics* 123.2-3 (2004), pp. 281–285.